

Focal adhesion kinase modulates tension signaling to control actin and focal adhesion dynamics

Markus Schober,¹ Srikala Raghavan,¹ Maria Nikolova,¹ Lisa Polak,¹ H. Amalia Pasolli,¹ Hilary E. Beggs,² Louis F. Reichardt,² and Elaine Fuchs¹

¹Howard Hughes Medical Institute, Laboratory of Mammalian Cell Biology and Development, The Rockefeller University, New York, NY 10021

²Department of Physiology, University of California, San Francisco, San Francisco, CA 94143

In response to $\alpha\beta 1$ integrin signaling, transducers such as focal adhesion kinase (FAK) become activated, relaying to specific machineries and triggering distinct cellular responses. By conditionally ablating *Fak* in skin epidermis and culturing *Fak*-null keratinocytes, we show that FAK is dispensable for epidermal adhesion and basement membrane assembly, both of which require $\alpha\beta 1$ integrins. FAK is also dispensable for proliferation/survival in enriched medium. In contrast, FAK functions downstream of $\alpha\beta 1$ integrin in regulating cytoskeletal dynamics and orchestrating polarized keratinocyte migration out

of epidermal explants. *Fak*-null keratinocytes display an aberrant actin cytoskeleton, which is tightly associated with robust, peripheral focal adhesions and microtubules. We find that without FAK, Src, p190RhoGAP, and PKL-PIX-PAK, localization and/or activation at focal adhesions are impaired, leading to elevated Rho activity, phosphorylation of myosin light chain kinase, and enhanced tensile stress fibers. We show that, together, these FAK-dependent activities are critical to control the turnover of focal adhesions, which is perturbed in the absence of FAK.

Introduction

Integrins are heterodimeric transmembrane adhesion receptors composed of α and β subunits, which serve, often in combination with receptor tyrosine kinases, to control cell adhesion, migration, proliferation, differentiation, and survival (Hynes, 2002; Miranti and Brugge, 2002; Schwartz and Ginsberg, 2002; Giancotti and Tarone, 2003). Together, these functions govern morphogenesis and tissue homeostasis and, when deregulated, contribute to tumorigenesis and cancers (Avizienyte et al., 2002; Hsia et al., 2003; Hannigan et al., 2005; McLean et al., 2005; Owens et al., 2005; Wu et al., 2005; Janes and Watt, 2006; Wilhelmson et al., 2006).

$\alpha 3\beta 1$, $\alpha 2\beta 1$, $\alpha 5\beta 1$, $\alpha v\beta 6$, and $\alpha 6\beta 4$ are all found in skin epidermis, where they bind to their ligands in the basement membrane and serve a diverse array of functions (Fuchs et al., 1997; Watt, 2002; Wilhelmson et al., 2006). Conditional targeting

of the genes encoding the hemidesmosomal integrins $\alpha 6$ and $\beta 4$ results in epidermal–dermal detachment, skin blistering, and defects in cell survival (Dowling et al., 1996; Georges-Labouesse et al., 1996; van der Neut et al., 1996), whereas targeted deletions of $\alpha 3$ and $\beta 6$ result in microblistering and wound defects, respectively (DiPersio et al., 1997). In contrast, $\beta 1$ ablation causes defects in epidermal–dermal attachment, basement membrane organization/assembly, hair follicle downgrowth/morphogenesis, and epidermal wound closure (DiPersio et al., 1997; Brakebusch et al., 2000; Raghavan et al., 2000; Grose et al., 2002).

$\alpha\beta 1$ integrins form focal adhesions (FAs), composed of a complex group of proteins and signaling molecules that associate with the actin and microtubule cytoskeletons and orchestrate these diverse functions. Primary $\beta 1$ -knockout (KO) epidermal keratinocytes can be cultured in vitro under conditions where they proliferate similarly to their wild-type (WT) counterparts (Raghavan et al., 2003). These keratinocytes display alterations in cell-matrix adhesion, enlarged, peripheral FAs, and robust actin stress fibers, suggestive of properties that might contribute to the perturbations in hair follicles and epidermal wound closure seen in vivo. However, the molecular mechanisms by which $\alpha\beta 1$ integrins control the diverse set of cell biological processes in epidermal keratinocytes remain largely unknown.

Correspondence to Elaine Fuchs: fuchs@rockefeller.edu

S. Raghavan's present address is College of Dental Medicine and Department of Dermatology, Columbia University, New York, NY 10032.

Abbreviations used in this paper: cKO, conditional KO; FA, focal adhesion; FN, fibronectin; GAP, GTPase-activating protein; ILK, integrin-linked kinase; KO, knockout; MK, mouse keratinocyte; MLC, myosin light chain; MYPT, myosin phosphatase target; PAK, p21-activated kinase; PIX, PAK-interacting exchange factor; PKL, p95 paxillin kinase linker; PXN, paxillin; PYK2, proline-rich tyrosine kinase 2; ROCK, Rho kinase; VIN, vinculin; WT, wild-type.

The online version of this article contains supplemental material

Integrins lack endogenous enzymatic activity and are thus believed to depend on signal transducers such as the nonreceptor kinases FAK, its sequence homologue proline-rich tyrosine kinase 2 (PYK2), or integrin-linked kinase (ILK), as well as a variety of scaffolding proteins that link integrins to the actin cytoskeleton to unfold their functions (Hynes, 2002). Upon integrin engagement with the extracellular matrix, FAK becomes activated and physically interacts with $\beta 1$'s cytoplasmic tail as well as with various signaling molecules at FAs (Schaller et al., 1995; Chen et al., 2000). In cultured $\beta 1$ integrin-null epidermal cells, FAK activity is markedly reduced, revealing FAK as a potential transducer of $\beta 1$ integrin's diverse activities in skin (Raghavan et al., 2003).

The notion that FAK-mediated $\beta 1$ integrin signaling controls these processes in the skin epidermis is suggested from *Fak* conditional gene targetings, which have revealed defects in basement membrane assembly and/or remodeling in developing dorsal forebrain (Beggs et al., 2003). However, although *Fak*-deficient fibroblasts exhibit restricted migration, endothelial cells and HeLa cells show increased motility (Ilic et al., 1995; Yano et al., 2004; Tilghman et al., 2005; Braren et al., 2006). Additionally, loss of FAK results in apoptosis in embryonic fibroblasts and endothelial cells, but not in meningeal fibroblasts (Ilic et al., 1995; Beggs et al., 2003; Shen et al., 2005; Braren et al., 2006). Whether cellular context accounts for these seemingly opposing findings is not yet clear.

Recently, *Fak* was conditionally targeted in postnatal mouse skin epithelium, revealing defects in hair follicles and sebaceous glands (Essayem et al., 2006) and resistance to tumorigenesis (McLean et al., 2004). However, the molecular and cellular mechanisms responsible for these phenotypes have yet to be elucidated, and the differences in KO strategies and genetic backgrounds preclude comparisons between *Fak* and $\beta 1$ conditional targetings. To unravel the relative importance of epidermal FAK in mediating downstream signaling functions of $\beta 1$ integrins, we have mated *Fak(fl/fl)* mice with the same *K14-Cre* recombinase mice that we used previously to target $\beta 1$ integrin. For these comparisons, we also derived primary epidermal keratinocytes from both *Fak*-null and $\beta 1$ -null skins.

We show that, in contrast to $\beta 1$ and distinct from some prior functions attributed to FAK, FAK is largely dispensable for epidermal adhesion, basement membrane organization, proliferation, survival, and terminal differentiation. Rather, FAK controls cytoskeletal dynamics and FA disassembly, and without it, keratinocytes are perturbed in their motility and their ability to polarize migration out of skin explants. Mechanistically, our data suggest that these defects are in part due to decreased phosphorylation of Src and p190RhoGAP (GTPase-activating protein), yielding increased Rho/Rho kinase (ROCK) signaling and inefficient recruitment of the p95 paxillin kinase linker-PAK-interacting exchange factor-p21-activated kinase (PKL-PIX-PAK) complex to FAs. Finally, we substantiate the biological significance of these activities downstream of $\alpha\beta 1$ integrin and FAK by inhibiting tension signaling with small molecule inhibitors and explore the consequences to FA dynamics.

Results

FAK is not required for integrin expression, basement membrane formation, or cell-substratum adhesion in skin epidermis

FAK activity has been found to depend on $\alpha\beta 1$ integrin signaling in the skin epidermis (Raghavan et al., 2003). To test the hypothesis that FAK functions as a key transducer of $\alpha\beta 1$ signaling in epidermis, we mated *K14-Cre* mice (Vasioukhin et al., 1999) to mice where the second kinase domain of *Fak* was flanked by loxP sites. Upon excision of floxed exons by Cre recombinase, an early stop codon is generated, ablating FAK protein expression (Beggs et al., 2003). Immunofluorescence microscopy documented specific loss of FAK in skin epithelium and not dermis, and this was further confirmed by immunoblot analyses (Fig. 1, A and B).

Although, at birth, *Fak* conditional KO (cKO) mice were phenotypically indistinguishable from WT littermates, their hair coat did not emerge on time (Fig. S1, A and B, available at <http://www.jcb.org/cgi/content/full/jcb.200608010/DC1>; Essayem et al., 2006). Histological analysis further revealed a defect in follicle downgrowth (Fig. S1 C). This defect appeared to be rooted in a failure of follicles to migrate downward, rather than alterations in proliferation and/or apoptosis (Fig. S1, D and E). Detection of such early neonatal defects was uniquely possible with *K14-Cre* mice, which embryonically ablate floxed genes in epidermis (Vasioukhin et al., 1999).

To determine whether FAK is required for integrin expression or basement membrane formation in skin, we first conducted immunofluorescence microscopy using antibodies against $\beta 1$ integrin, expressed in dermal fibroblasts and basal epidermal cells, and laminin 5, the primary ECM ligand for epidermal integrins and a major component of the basement membrane at the dermal-epidermal boundary. These labeling patterns were indistinguishable between WT and FAK-deficient skin (Fig. 1 C). Ultrastructural analyses further revealed an intact basement membrane, accompanied by structurally normal $\alpha 6\beta 4$ integrin-containing hemidesmosomes of comparable length and density (Fig. 1, D and E). An explanation of the box-and-whisker diagram (Tukey, 1977) used to graphically display the spread of these data can be found in Fig. S2 (available at <http://www.jcb.org/cgi/content/full/jcb.200608010/DC1>).

We next used FACS analyses to quantify integrin surface levels on freshly isolated epidermal keratinocytes (Fig. 1 F). Normal surface levels of $\beta 1$, $\beta 4$, $\alpha 2$, $\alpha 6$, αv , and $\beta 6$ integrins were observed, indicating that loss of FAK did not affect integrin expression. Moreover, as judged by FACS with an antibody specific for activated $\beta 1$ integrin, no differences were noted in the activity of $\alpha\beta 1$ integrins in the absence of FAK. Consistent with these observations, WT and *Fak*-null epidermal cells adhered similarly to a variety of purified ECM substrates of the underlying basement membrane (Fig. 1 G). Collectively, these studies suggest that FAK functions in the subset of $\alpha\beta 1$ integrin functions required for hair follicle morphogenesis, but it is dispensable for basement membrane assembly, integrin expression, adhesion, and tissue homeostasis.

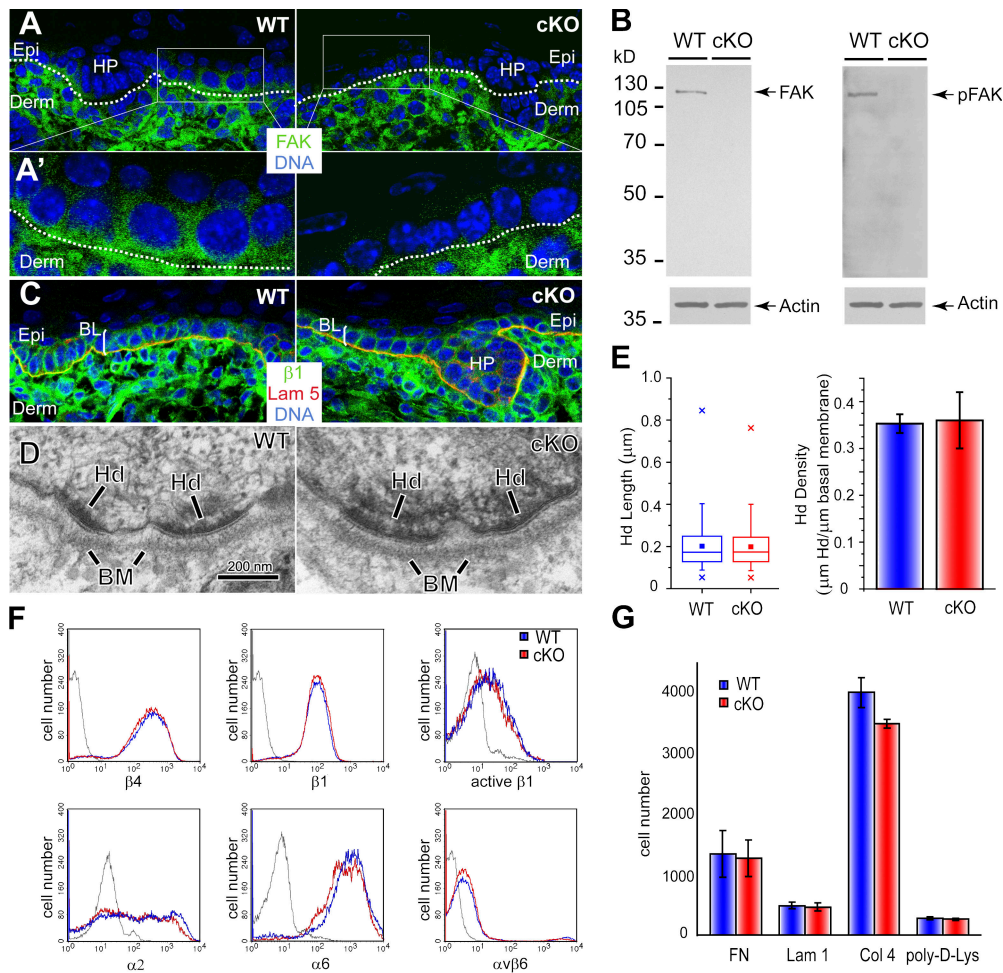


Figure 1. Intact basement membrane, surface integrins, and cell adhesion in keratinocytes lacking FAK. (A, A', and C) FAK and the dermo-epidermal junction. Newborn WT and *K14-Cre/Fak^{fl/fl}* cKO skin sections were subjected to immunofluorescence microscopy with the antibodies shown. Antibodies are color coded according to secondary antibodies. Dotted line demarcates the boundary between epidermis (Epi) and dermis (Derm). Areas in white boxes (A) are magnified in A'. $\beta 1$, $\beta 1$ integrin; Lam 5, laminin 5; DNA, DAPI staining; HP, hair placode; BL, basal layer. (B) Immunoblot of epidermal cell lysates. Blots were probed with the following antibodies: FAK, pY397-FAK (p-FAK), and β -actin (loading control). (D) Transmission EM (TEM) showing representative examples of WT and cKO epidermal-dermal borders. Note comparable morphology, size, and density of hemidesmosomes (Hd). BM, basement membrane. (E) Hemidesmosome length and frequency are not affected by loss of FAK. Box-and-whisker diagrams at left display the distribution of the data: mean (square), 25th percentile (bottom line), median (middle line), 75th percentile (top line), 5th and 95th percentile (whiskers), and minimum and maximum measurements (x). (See Fig. S2, available at <http://www.jcb.org/cgi/content/full/jcb.200608010/DC1>, for additional information.) Graph at right shows analyses of total micrometers of hemidesmosome per micrometer of basal plasma membrane. (F) FACS quantification of epidermal integrin surface levels. Surface-specific integrin antibodies used are indicated at bottom of each graph. Active $\beta 1$ corresponds to a surface antibody that specifically recognizes the active configuration of $\beta 1$, irrespective of α partner. Gray line indicates secondary antibody-only control. (G) Adhesion assays were performed as described in Materials and methods. Note comparable adhesion of WT and cKO keratinocytes to FN, laminin 1, collagen 4, and poly-D-lysine substrates. Error bars reflect SD of triplicate experiments.

Primary *Fak*-null keratinocytes grow in culture but exhibit enhanced sensitivity to serum starvation

To probe for molecular and biological functions of FAK in epidermal keratinocytes, we cultured primary keratinocytes on fibroblast feeder layers (Fig. 2). *Fak* KO keratinocytes were propagated over multiple passages without major growth defects, and feeder cells could be withdrawn upon passaging. However, these cells appeared to be more sensitive to serum starvation than WT keratinocytes. Thus, on fibronectin (FN)-coated dishes, MAPK activity, as measured by p42/44 phosphorylation, was reduced in serum-starved *Fak* KO, as compared with either starved WT or serum-stimulated KO or WT keratinocytes.

In contrast, the phosphorylation of other signaling molecules such as AKT appeared unchanged.

FAK- and $\beta 1$ -deficient epidermal cultures differ in their PYK2 and ILK activities, but both display alterations in cell shape

We next examined whether *Fak* ablation affected the activity and/or subcellular localization of the two other $\beta 1$ signal transducing, nonreceptor kinases, PYK2 and ILK (Hannigan et al., 1996; Astier et al., 1997; Gismondi et al., 1997). In the absence of FAK, Pyk2 was slightly hyperphosphorylated, but phospho-Pyk2 still localized to *Fak*-deficient FAs. ILK levels and localization were similar between WT and *Fak* KO

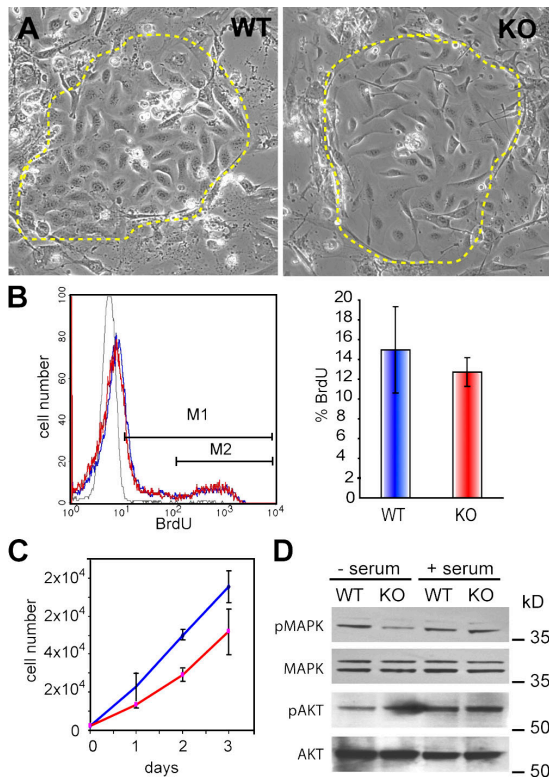


Figure 2. *Fak*-null keratinocytes proliferate well under optimal growth conditions. Primary MKs were cultured from *Fak* cKO and WT epidermis on a fibroblast feeder layer (A). Once colonies formed, feeders were selectively removed with Versene, and MKs were passaged in the absence of feeders for the subsequent studies (B–D). (A) Phase-contrast images of representative WT and *Fak* KO colonies on feeders. (B) Cell cycle analyses. BrdU was administered to the culture medium for 4 h followed by harvesting and FACS analyses. Note comparable cell cycle profiles and BrdU incorporation. (C) Growth curves. MKs were plated in serum-containing medium, and thereafter cells were harvested daily in triplicate and cells were counted. Error bars indicate SD. (D) Immunoblot analyses of MK lysates cultured in the presence or absence of serum for 24 h before harvesting. Antibodies used are shown at left; molecular masses of band sizes are indicated at right in kD.

keratinocytes (Fig. 3 A). In contrast, activated FAK and PYK2 were markedly reduced in $\beta 1$ -null keratinocytes, where some delocalization of ILK from FAs was also noted (Fig. 3 B). PYK2/ILK signaling was still at least partially maintained in *Fak* KO cells; however, rhodamine-phalloidin labeling revealed marked defects in actin organization and cell spreading, resembling those seen in $\beta 1$ -null keratinocytes.

To investigate these defects in greater detail, we plated keratinocytes on FN-coated glass dishes, fixed and stained them at multiple intervals, and quantified the contact area between the cell and its underlying substratum (Fig. 4). In the absence of FAK, actin cables lined cell boundaries, while atypically dense bundles of actin stress fibers converged at FAs, often crossing intracellularly at multiple sites. This was in striking contrast to WT keratinocytes, which displayed organized actin networks, with relatively modest stress fibers converging in parallel arrays at peripheral FAK-positive FAs. These defects were accompanied by marked abnormalities in the rate and extent of spreading in FAK-deficient cells. As depicted in the box-and-whisker diagrams, the perturbations in cell shape and spreading became

more pronounced over time, as did the range of effects observed (Fig. 4 B and Fig. S2).

To further investigate the root of FAK-dependent changes in cytoskeletal architecture and cell shape/spreading, we counterstained rhodamine-phalloidin labeled keratinocytes with antibodies against the FA molecules vinculin (VIN) and paxillin (PXN). VIN and PXN localized at the sharp, constricted cellular apices that were closely associated with massive bundles of actin fibers lining the periphery of aberrantly shaped *Fak*-deficient keratinocytes (Fig. 5, A and B). Although peripheral FAs exhibited markedly enhanced staining intensity and area in FAK-deficient cells, the smaller and more weakly stained central FAs were largely absent (Fig. 5, C and D). Defects in cell shape; actin organization; and FA size, distribution, and intensity were largely restored after reexpressing FAK in *Fak* KO keratinocytes (Fig. 5, E–G). These data underscore the importance of FAK in FA regulation and actin organization.

FAK promotes cytoskeletal dynamics and FA turnover

To examine actin–FA dynamics in real time, we first mated *K14-Cre, Fak(fl/fl)* mice on the background of previously generated *K14-GFPactin* transgenic mice (Vaezi et al., 2002) and then transfected *Fak*-null and WT *K14-GFPactin* keratinocytes with an *RFPzyxin* expression vector (Bhatt et al., 2002; Raghavan et al., 2003). Video microscopy revealed a considerably more static actin cytoskeleton and associated FAs in *Fak*-null keratinocytes relative to their WT counterparts (Fig. 6, A and B and Video 1, available at <http://www.jcb.org/cgi/content/full/jcb.200608010/DC1>). Most WT keratinocytes extended lamellipodia uniformly around their circumference, and as they formed, lamellipodia seeded numerous focal complexes connected by short, thin actin bundles (Fig. 6 A). A few of these focal complexes slowly developed into more robust FAs, which then served as convergence sites for larger stress fibers. In contrast, *Fak*-null keratinocytes formed lamellipodia primarily around existing robust FAs, with new focal complexes maturing rapidly into atypically large peripheral FAs associated with unusually thick actin cables (Fig. 6 A and Videos 1 and 2).

WT keratinocytes displayed dynamic FAs, which were continually drawn toward the cell center (Fig. 6 B and Video 1). In contrast, the large FAK-deficient FAs accumulated at cell edges for extended times (Fig. 6 B and Video 2). After prolonged periods of cellular tugging, retractive forces often caused abrupt release of associated cellular contacts with the substratum, resulting in rapid, uncoordinated changes in FAK KO morphology (Videos 1 and 2).

To assess differences in the kinetics of FA dynamics, we monitored individual FAs in keratinocytes transfected with GFP-PXN and calculated the rate constants for both FA assembly and disassembly (Webb et al., 2004). Although FA assembly rates were only slightly lower in *Fak* KO versus WT keratinocytes, disassembly rates were significantly decreased (Fig. 6 C). This was further substantiated by FRAP experiments, where a significant increase was noted in the half-times of fluorescence recovery after photobleaching (Fig. 6 D). In contrast, the mobile fraction of GFP-PXN appeared unaffected

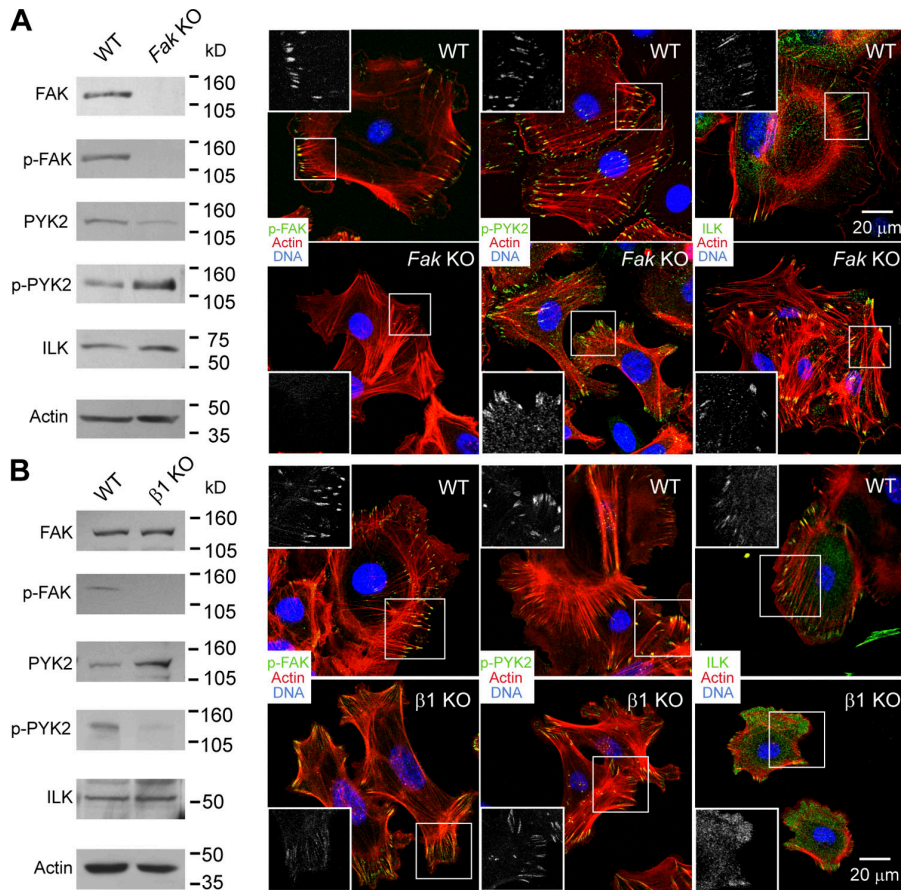


Figure 3. PYK2 and ILK still localize to FAs in *Fak*-null keratinocytes. Immunoblot analysis and immunofluorescence of WT and *Fak* KO MK (A) or WT and $\beta 1$ KO MK (B). Antibodies used are as shown, except phalloidin (red) is used to mark F-actin, and DAPI (blue) labels nuclear chromatin. Phosphorylated versions of FAK and PYK2 are active. Antibodies are color coded according to the secondary antibodies used. Boxed areas are magnified and shown as insets in which phalloidin fluorescence has been omitted. Note that *Fak* KO MKs still display active PYK2 as well as FA-localized ILK.

by the status of FAK (Fig. 6 E). These data provide compelling evidence that the large FAs in FAK-deficient keratinocytes arise from a defect in FA disassembly.

FAK functions in organizing and polarizing actin networks to facilitate efficient, coordinated cell migration

The observed defects in FA disassembly and cytoskeletal organization led us to posit that FAK may function in promoting directed cell migration. We tested this possibility by first generating tissue explants from *K14-GFPactin*, WT, and *Fak*-cKO skins placed on FN-coated glass dishes and then monitoring the outgrowth of interconnected epithelial sheets of GFPactin-expressing keratinocytes from these explants (Vaezi et al., 2002). Quantification revealed a marked delay in the outgrowth from *Fak* cKO explants compared with WT explants (Fig. 7, A and B), whereas lamellipodial activity appeared similar between WT and KO explants (Video 3, available at <http://www.jcb.org/cgi/content/full/jcb.200608010/DC1>).

WT explants polarized their actin cytoskeleton, exhibiting parallel actin bundles that were oriented perpendicularly to the leading edge of the outgrowing cells (Fig. 7, C and D). Antibodies against E-cadherin, which mark stable cell-cell contacts, underscored the elongated, polarized character of these epidermal sheets. Actin fibers associated with PXN-labeled FAs were also distributed evenly and unidirectionally oriented toward the leading edges of the outgrowing WT explants.

In contrast, *Fak*-null epidermal explants exhibited a seemingly random orientation of actin bundles, often crossing at multiple places, whereas enlarged FAs pointed in different directions in disoriented cells at the leading edge (Fig. 7, C and D).

A priori, the differences in explant outgrowth could be due solely to a failure to coordinate cytoskeletal dynamics across the outgrowing epithelial sheet. Alternatively, it could be that the defects in outgrowth stem from intrinsic defects in the migration of individual cells, which subsequently fail to coordinate directed movements within the outgrowing sheet. To assess the motility of individual keratinocytes, equal numbers of WT and KO keratinocytes were seeded in the top compartment of Boyden chambers and assayed for the number of cells that migrated through the filter to the FN matrix located in the chamber below. Quantification revealed that the number of WT cells migrating through the filter was approximately five times higher than the number of KO cells (Fig. 7 E). These data suggest that FAK promotes FA dynamics and directed migration in keratinocytes and supports the polarized, unidirectional migration of epithelial sheets at the wound edge.

FAK is not required for microtubule targeting to FAs

The migration defects arising from loss-of-function FAK mutations pointed to a major role for FAK in regulating FA dynamics for the purpose of orchestrating cytoskeletal organization

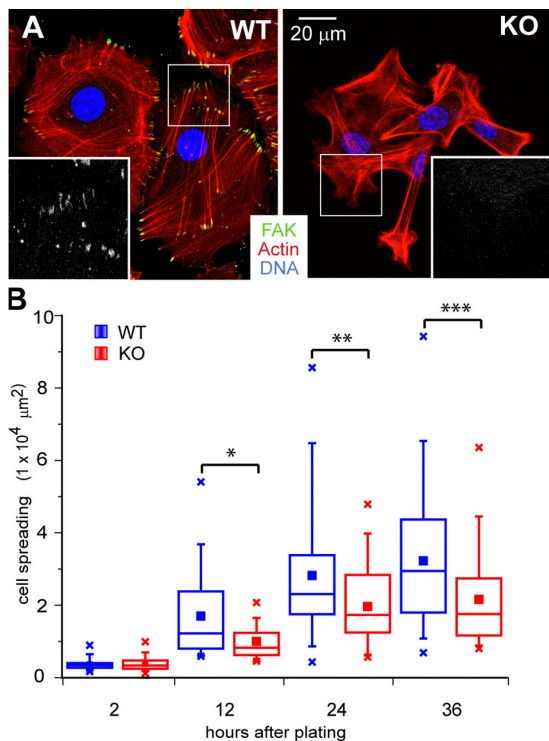


Figure 4. Keratinocytes lacking FAK display an exaggerated FA-actin stress fiber network and constricted cell morphology. (A) Immunofluorescence microscopy of representative MKs from WT and *Fak* cKO epidermis spread on FN for 48 h and labeled with anti-FAK (green), phalloidin (red), and DAPI (blue). Boxed areas are magnified in insets, which show only anti-FAK staining. (B) Box-and-whisker plot of cell spreading kinetics, indicating the mean (squares), 25th percentile (bottom line), median (middle line), 75th percentile (top line), 5th and 95th percentile (whiskers), and minimum and maximum measurements (x). Morphometric analyses of cell spreading were performed by measuring the average contact area between the cell and its substratum in square micrometers described in box-and-whisker diagrams. $n \geq 60$ cells per time point. Asterisks indicate significant differences between WT and KO (*t* test). Note that differences in spreading increased over time. *, $P = 0.025$; **, $P = 0.0018$; ***, $P = 0.0006$.

and cellular movements. Increasing evidence has implicated microtubule targeting to FAs as an initial step in FA turnover (Bershadsky et al., 1996; Kaverina et al., 1998, 1999; Small et al., 2002; Ezratty et al., 2005). To assess whether microtubule targeting to FAs might be altered by FAK deficiency, we used immunofluorescence and video microscopy to examine microtubule networks. In WT keratinocytes, microtubules formed a regular array around the nucleus and projected toward the cell periphery (Fig. S3, available at <http://www.jcb.org/cgi/content/full/jcb.200608010/DC1>). In *Fak*-null keratinocytes, this organization was perturbed, and the majority of microtubules pointed toward the robust FAs that were associated with massive stress fibers. Time-lapse analyses of keratinocytes transfected with either GFP-tubulin (Video 4) or a GFP-tagged plus-end microtubule binding protein (β 1; Video 5) further indicated that dynamic microtubules target robust, peripheral FAs, resulting in an altered distribution of the microtubule cytoskeleton in the absence of FAK.

Collectively, our data suggest that FAK modulates FA dynamics in mouse epidermal keratinocytes but it is not essential

for the targeting of dynamic microtubules to FAs. Additionally, as microtubule targeting is thought to promote FA turnover, the presence of microtubules at FAK-deficient FAs implies that, whatever the mechanism involved in microtubule-mediated FA turnover, it is dysfunctional in the absence of FAK. This result supports previous observations where FAK-deficient embryonic fibroblasts do not disassemble FAs when microtubules repolymerize in response to washout of the microtubule depolymerizing drug nocodazole (Ezratty et al., 2005).

***Fak*-null FAs fail to recruit and activate p190RhoGAP and PAK**

The main characteristic of *Fak* KO keratinocytes is robust FAs, which are tightly associated with prominent stress fibers. Elevated Rho activity can result in elevated stress fiber formation and stabilization of FAs (Chrzanowska-Wodnicka and Burridge, 1996), whereas RhoA inactivation by p190RhoGAP can promote cell spreading and migration (Arthur and Burridge, 2001). Furthermore, FAK has been associated with the transient suppression of Rho activity during cell spreading (Ren et al., 2000) and it has been speculated that FAK may cooperate with β 1 integrin and Src tyrosine kinase to phosphorylate and activate p190RhoGAP at FAs (Fincham et al., 1999; Arthur et al., 2000; Dumenil et al., 2000; Brouns et al., 2001).

To test this hypothesis, we first assessed Src activity in FN-stimulated keratinocytes grown in the presence or absence of serum. Immunoprecipitation of Src followed by anti-pY418-Src immunoblot analysis revealed a marked reduction of phosphorylated (active) Src in *Fak*-null keratinocytes grown under serum-free conditions where Src activation is likely to emanate primarily from integrin activation (Fig. 8 A). As shown by its faster electrophoretic mobility, Src was mostly unphosphorylated (inactive). In contrast, no considerable changes in the status of Src were noted in cells cultured in the presence of serum, where Src activation can additionally occur through ligand-mediated engagement of transmembrane tyrosine kinase receptors. These results agree with the previously established requirement of FAK autophosphorylation for efficient recruitment of Src to FAs (Schaller et al., 1994).

We assessed the status of p190RhoGAP by immunoprecipitating it from total cell lysates and conducting an anti-phosphotyrosine (p-Tyr) immunoblot analysis. p190RhoGAP was hypophosphorylated in *Fak* KO cells grown without serum, whereas comparable amounts of tyrosine-phosphorylated p190RhoGAP were detected when serum was present (Fig. 8 B). The requirement for FAK in phosphorylating and activating both Src and p190RhoGAP at integrin activation sites provides an underlying mechanism for the convergence of robust actin fibers at sites of FAs in *Fak* KO keratinocytes.

RhoGTP can activate ROCK, resulting in the phosphorylation and inactivation of the regulatory subunit of myosin light chain (MLC) phosphatase (myosin phosphatase target [MYPT]), leading in turn to increased phosphorylation and activation of MLC and stress fiber formation (Matsumura, 2005). To test whether this tension-signaling pathway is hyperactivated in *Fak*-null keratinocytes, we examined the levels and phosphorylation status of MYPT and MLC (Fig. 8 C). Although total

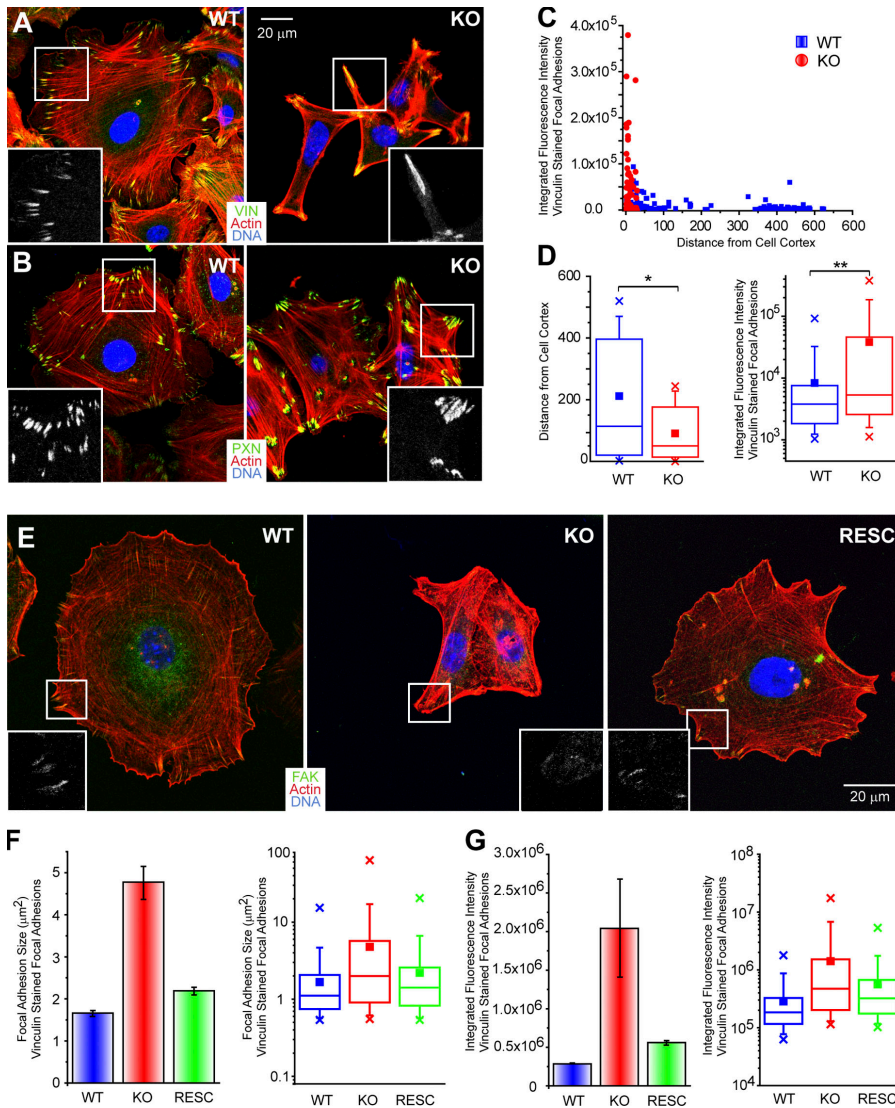


Figure 5. FAK-dependent differences in FA size and distribution. (A and B) Immunostaining of WT and *Fak*-KO keratinocytes for actin (red), nuclear chromatin (DAPI; blue), and FA markers VIN and PXN (green). (C) Scatter plot indicating the integrated fluorescence intensity of VIN-labeled FAs and their relative position from the cell cortex. (D) Box-and-whisker diagrams describing the distribution of FAs from the cortex to the center and the relative fluorescence intensity of VIN-labeled FAs. Box-and-whisker plots indicate the mean (squares), 25th percentile (bottom line), median (middle line), 75th percentile (top line), 5th and 95th percentile (whiskers), and minimum and maximum measurements (x).*, $P = 0.00003$; **, $P < 0.00001$ (*t* test). (E–G) Retroviral infection and expression of recombinant FAK rescued the defects in actin cytoskeleton and FA size and distribution. (E) Immunostaining of representative WT, *Fak*-KO, and FAK-rescued *Fak*-KO MKs with anti-FAK (green), phalloidin (red), and DAPI (blue). Insets show FAK staining, absent in KO but restored in FAK-rescued KO cells. (F and G) Quantitative analysis on VIN-stained KO, WT, and KO cells reexpressing FAK (RESC) show that the size of KO FAs and their relative VIN staining intensity was restored upon reexpression of FAK in KO keratinocytes. Error bars indicate SEM.

MYPT levels appeared to be slightly reduced, MYPT was hyperphosphorylated (inactive) at its ROCK-sensitive threonine residue. The outcome of these changes appeared to be a small but statistically significant increase in the total levels of active pMLC, as judged not only by immunoblot analysis but also quantitative immunofluorescence microscopy (Fig. 8, C–E). Moreover, in WT cells, anti-pMLC decorated the central actin fibers as well as the cortical actin network, whereas in *Fak* KO cells, anti-pMLC displayed a more robust decoration of the massive stress fiber network.

To determine whether this increase in Rho/pMLC-mediated tension is attributable to the spreading defects of *Fak* KO keratinocytes and/or their defective FA dynamics, we treated keratinocytes with the ROCK inhibitor Y-27632, the myosin inhibitor blebbistatin, and the MLC kinase (MLCK) inhibitor ML7, and then conducted immunofluorescence microscopy and quantitative relative integrated fluorescence intensity analyses to evaluate the effects on cell spreading, FA size, and FA localization. As shown in Fig. 9 (A and B), the differences in WT versus KO keratinocyte spreading were largely ameliorated by Y-27632 and blebbistatin, and to a lesser extent by ML7.

Quantitative analyses of FA staining intensity are shown in Fig. 9 C (see also Fig. S4, available at <http://www.jcb.org/cgi/content/full/jcb.200608010/DC1>). These data further revealed that the statistical distribution of FAs in KO keratinocytes, which was highly skewed toward larger, more intensely stained FAs (mock), was significantly restored to normal upon treatment with these RhoA/tension-relieving drugs. In contrast, treatment with nocodazole, which depolymerizes microtubules and enhances Rho activity, resulted in increased FA size and VIN staining intensity even in KO cells. Quantitative analyses further revealed a clear shift in the distribution of FAs to a more peripheral location (Fig. S4).

Fak-null focal contacts are defective at activating PAK

MLCK can be phosphorylated and inhibited by PAK (Sanders et al., 1999), which has recently been proposed to form a complex with PKL, βPIX, and PXN at FAs (Turner et al., 1999; West et al., 2001; Nayal et al., 2006). To test whether the function of this complex might require FAK activity, we first examined the relative levels of PKL, βPIX, and PAK. As judged

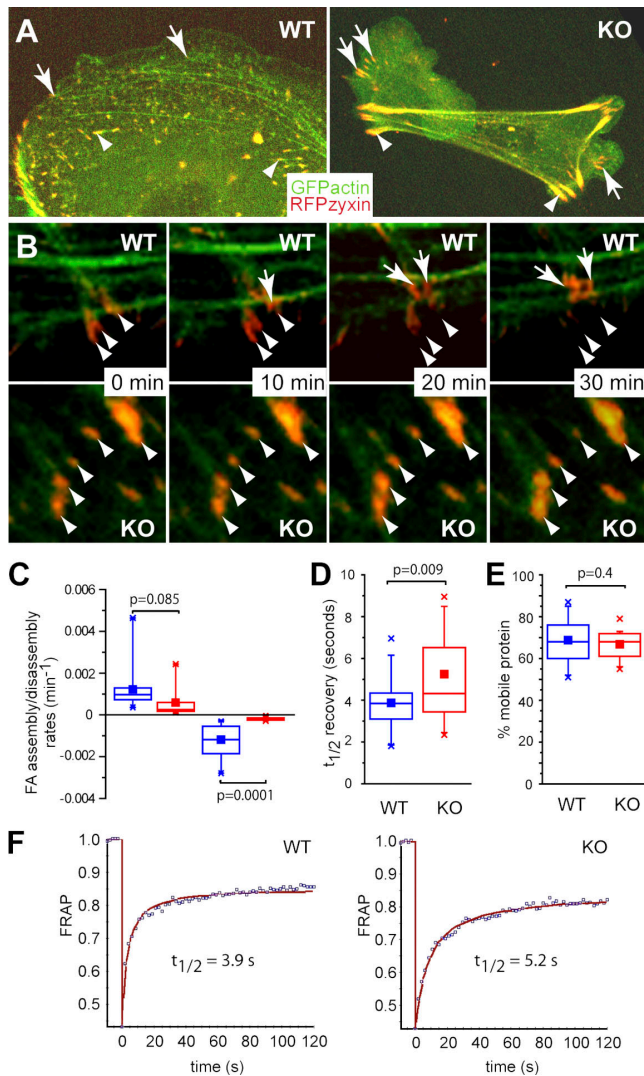


Figure 6. FAK promotes FA disassembly. Time-lapse images of primary MKs expressing K14-GFPactin (green) and RFPzyxin (red) to mark F-actin and FAs, respectively. (A) WT and KO cells generate broad lamellipodia and seed focal complexes (arrows). In KO MKs, lamellipodia formed preferentially at sites peripheral to the aberrant networks of stress fibers and enlarged FAs (arrowheads). This resulted in a more constricted cell shape. (B) Atypically thick actin bundles (green) converged at enlarged and less dynamic FAs in *Fak* KO MKs. Arrowheads mark FA position at 0 min. Note that FAs typically retract (arrows) after 30 min, but in KO MKs, FAs often remained at the same position for extended times. (C) Box-and-whisker diagram describing the differences in FA assembly and disassembly between WT and KO MKs. Box-and-whisker plots indicate the mean (squares), 25th percentile (bottom line), median (middle line), 75th percentile (top line), 5th and 95th percentile (whiskers), and minimum and maximum measurements (x). (D and E) Box-and-whisker diagrams describing the differences in half-time of FRAP and the mobile fraction of GFP-PXN between WT and KO MKs. $n \geq 5$ adhesions on 10 individual cells. (F) Representative photobleaching and recovery kinetics of GFP-PXN in WT and KO MKs.

by immunoprecipitation and immunoblot analyses, PKL was markedly reduced in KO keratinocytes (Fig. 10 A). This was confirmed by immunofluorescence microscopy where anti-PKL labeled WT FAs but was only weakly detectable at KO FAs (Fig. 10 B). This difference was substantial, as KO FAs are considerably larger and thus would have otherwise been expected to label more strongly with PKL.

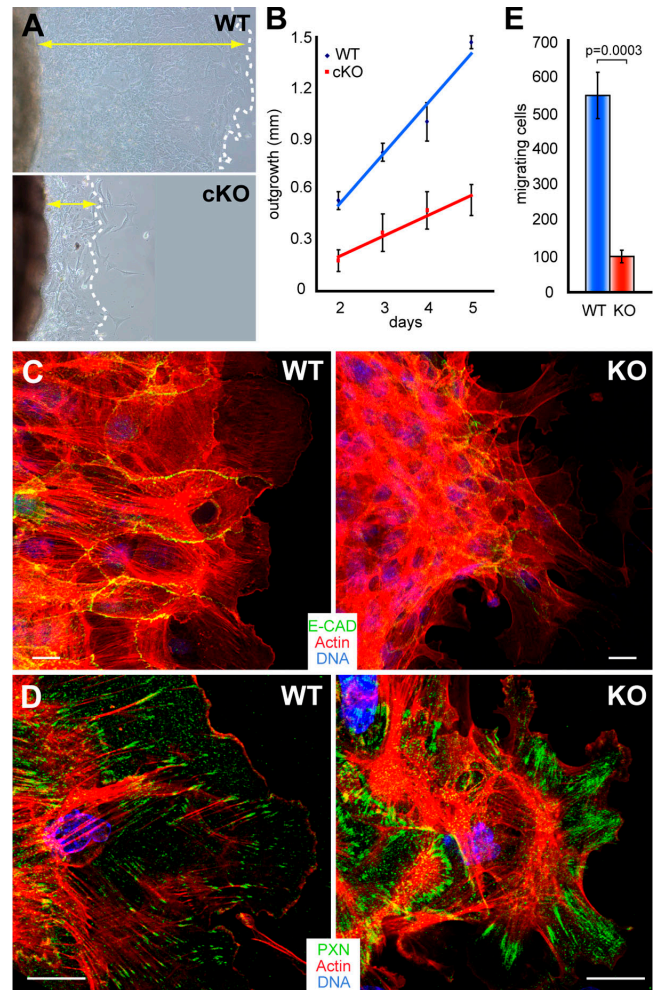


Figure 7. FAK controls cytoskeletal organization and directed migration from skin explants. (A) Phase-contrast images of WT and cKO skin explants (brown; left). The epidermal outgrowth from FAK-deficient explants (cKO) is severely decreased compared with WT explants. White dotted lines mark leading edges; yellow arrows denote distance between explant and its leading edge. (B) Quantification of epidermal outgrowth from skin explants. Mean of three independent experiments \pm SD. (C and D) Immunostaining for actin (red) and either E-cadherin (green) or PXN (green) reveals that cells, actin fibers, and FAs are highly polarized and oriented toward the leading edge in WT but not cKO explants. Bars, 20 μ m. (E) *Fak* KO MKs exhibit a markedly reduced ability to migrate from the top to the bottom compartment of a Boyden chamber containing fibroblast conditioned medium. Mean of three independent experiments \pm SD. $P = 0.0003$, two-tailed t test.

By immunoblot analyses, overall levels of β PIX and PAK appeared to be largely unaffected by *Fak* deficiency (Fig. 10 A). However, even though β PIX localization appeared normal, PAK localization was markedly altered in *Fak* KO keratinocytes (Fig. 10 B). Rather than the strong anti-PAK labeling of FAs in WT keratinocytes, anti-PAK labeling was largely diffuse in FAK-deficient cells and appeared reduced in intensity over KO FAs. Moreover, when we examined the status of activated (phosphorylated) PAK, we found that anti-phospho-PAK (p-PAK) labeled WT FAs but was barely detected in *Fak*-null FAs and largely diffuse throughout the cytoplasm (Fig. 10 B). Based on these data, we conclude that PAK was neither recruited nor activated efficiently at FAs in the absence of FAK.

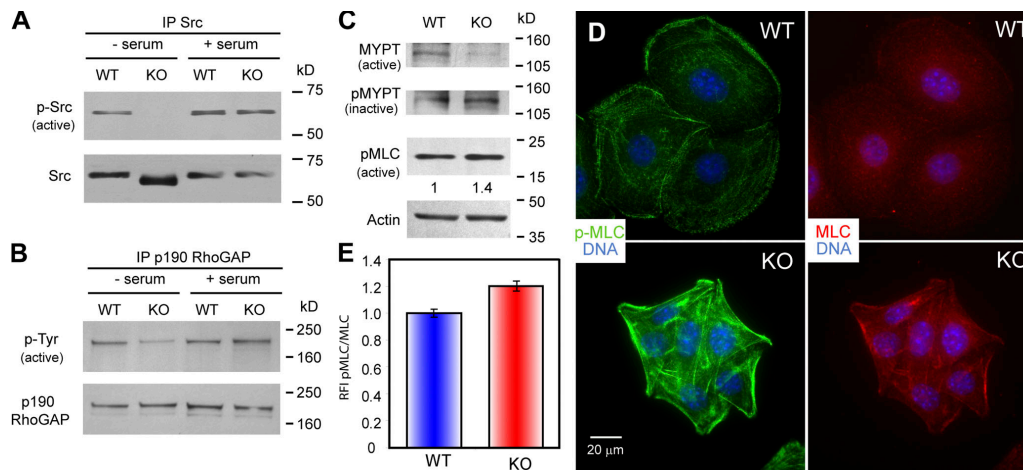


Figure 8. **FAK regulates p190RhoGAP and Rho/ROCK signaling.** (A–C) Immunoprecipitation and immunoblot analyses of tyrosine phosphorylation status of Src (pY418-Src) in MKs cultured in the presence or absence of serum/growth factors (A); tyrosine phosphorylation of p190RhoGAP in serum-starved *Fak* KO MKs (B); and phosphorylation of the regulatory subunit of MLC phosphatase (MYPT) and MLC (pMLC), reflective of increased Rho/ROCK mediated tension (C). (D and E) Enhanced pMLC in *Fak* KO versus WT MKs. Immunofluorescence microscopy of representative cells labeled with phosphorylated MLC antibodies (pMLC; pSer 19 MLC; green), MLC antibodies (MLC; red), and nuclear chromatin (DAPI; blue). Quantitative ratio imaging of pMLC and MLC indicates elevated pMLC levels in WT versus KO keratinocytes. ($P = 1.59E-05$, two-tailed t test; $n \geq 52$ cells). Error bars indicate SEM.

Discussion

FAK versus $\alpha\beta 1$ signaling in epidermal keratinocytes and skin explants

Of central importance to most cells is the ability to balance proliferation and differentiation, control adhesion to an underlying substratum, and when necessary, remodel this substratum and migrate in a directed fashion. These functions are particularly central to the mitotically active epidermal cell, which must continually undergo proliferation, detachment, and differentiation in the course of homeostasis, and upon injury, proliferate and migrate toward and repair the wound. Such movements are also important in hair follicle morphogenesis and cycling. The $\alpha\beta 1$ integrins and their orchestrated association with the actin and microtubule cytoskeletons play a crucial role in these processes, and their downstream signal transducers are thought to contribute heavily to these events.

For the present study, we established a system that allowed us to directly compare the relative contributions of FAK to the many diverse functions of $\alpha\beta 1$ integrins in the epidermis. Our studies provide compelling evidence that although $\alpha\beta 1$ integrins are known to function broadly in cell adhesion, basement membrane assembly and organization, tissue homeostasis, and balancing growth and differentiation, FAK is selectively involved in efficient cell spreading, regulation of FA and cytoskeletal dynamics, and directed migration (Fig. S5 A, available at <http://www.jcb.org/cgi/content/full/jcb.200608010/DC1>). When our present data are coupled with our previous observation that FAK is hypophosphorylated in $\beta 1$ KO keratinocytes (Raghavan et al., 2003), we could position FAK activation downstream of $\alpha\beta 1$ signaling and upstream of this subset of cellular functions.

PYK2 localized to the FAK-deficient FAs. However, in contrast to the $\beta 1$ -deficient FAs, PYK2 was still phosphorylated in the absence of FAK. Hence, we surmise that some of the

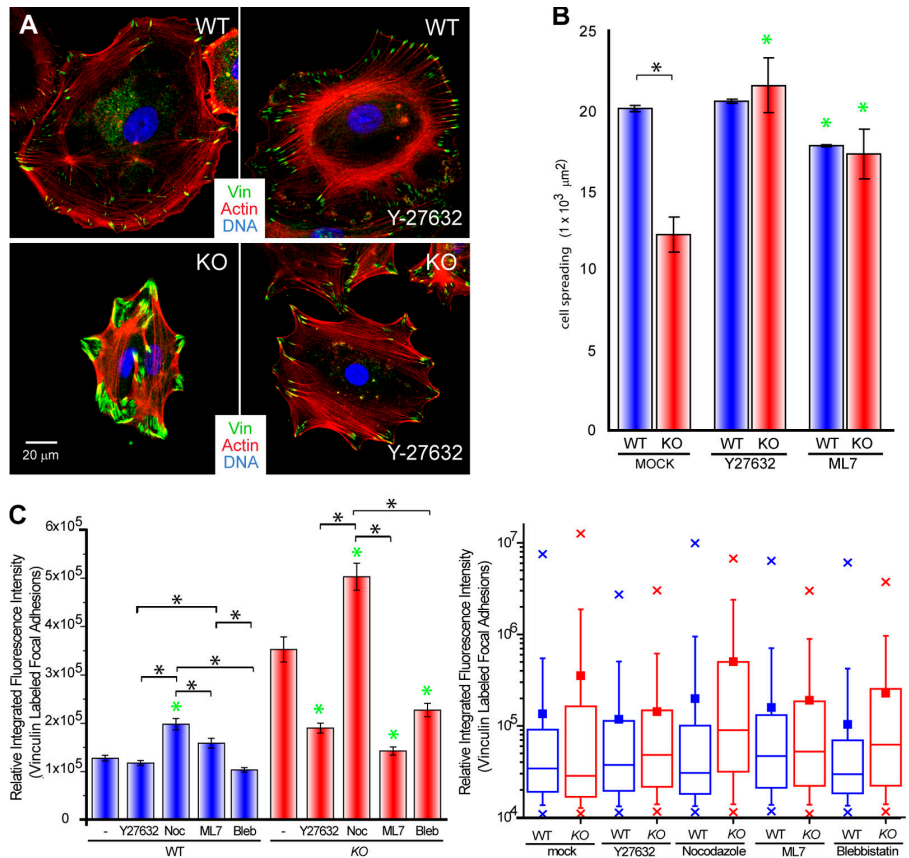
more global alterations seen in $\beta 1$ KO cells may reflect the loss of overlapping but discrete subsets of signaling functions mediated through FAK and PYK2. Additionally, although ILK was still expressed comparably, its localization in $\beta 1$ -null keratinocytes was diffuse, suggesting that one or more of its functions (Legate et al., 2006) may be selectively compromised in the $\beta 1$ -null but not *Fak*-null state.

FAK-related activation, signal transduction, small GTPase regulation, and tension signaling

Our loss-of-function studies in keratinocytes revealed that Rho/ROCK signaling was hyperactive in the absence of FAK, as reflected by increased MLC phosphorylation and massive cortical stress fiber bundles, which converged on large, peripheral FAs. The enhanced Rho activity in *Fak*-null keratinocytes implies that FAK indirectly or directly must either activate RhoGEFs (guanine nucleotide exchange factors) or repress RhoGAPs (Etienne-Manneville and Hall, 2002). In neural development and in fibroblasts, p190RhoGAP can be phosphorylated and activated in response to integrin and Src signaling to temper RhoA activation and promote cell spreading and migration (Arthur and Burridge, 2001; Billuart et al., 2001; Brouns et al., 2001). Consistent with this notion, *p53/Fak*-null fibroblasts are not able to suppress Rho activity during cell spreading (Ren et al., 2000).

Our data unveil an essential role for FAK in activating Src and p190RhoGAP upon integrin engagement. Thus, in keratinocytes, FAK is required for integrin/Src-dependent p190RhoGAP phosphorylation, suggesting a model where FAK/Src-induced phosphorylation of p190RhoGAP at FAs might locally promote RhoGTP hydrolysis to suppress Rho-induced stress fiber formation and FA stabilization (Fig. S5 B). Although we were unable to establish a physical association between endogenous p190RhoGAP and FAK

Figure 9. Interaction between FAK and tension-signaling components determines FA size and localization. (A and B) WT and KO MKs were plated on FN for 12 h before a 12-h treatment with the ROCK inhibitor Y27632 or the MLCK inhibitor ML7. Mean of three independent experiments \pm SD. Immunofluorescence microscopy (A) and quantitative analyses (B) show that ROCK or MLCK inhibition relaxes the constricted actin cytoskeleton, suppresses robust FAs marked by VIN, and promotes cell spreading in KO MKs. Black asterisks indicate significant differences between WT and KO ($P \leq 0.05$), and green asterisks indicate significant difference of treated cells from untreated cells ($P \leq 0.05$). (C) Box-and-whisker plots showing the relative integrated fluorescence intensity of VIN-stained FAs in the presence of 5 μ M Y27632, 5 μ M nocodazole, 5 μ M ML7, or 2 μ M blebbistatin. Box-and-whisker plots indicate the mean (squares), 25th percentile (bottom line), median (middle line), 75th percentile (top line), 5th and 95th percentile (whiskers), and minimum and maximum measurements (x). $n \geq 10$ for each condition. Green asterisks indicate significant differences ($P \leq 0.05$) of treated cells from untreated cells, and black asterisks indicate significant differences ($P \leq 0.05$) between treatments by analysis of variance and Tukey post hoc test.



(unpublished data), FAK has been shown to bind p190RhoGAP and phosphorylate it in vitro (Holinstat et al., 2006). When coupled with the biochemical interactions between these molecules, the FAK, Src, and integrin loss-of-function analyses provide a tight molecular link between Fak/Src-mediated integrin signaling and the regulation of Rho activity via p190RhoGAP.

Rho activity can result in elevated stress fiber formation and stabilization of FAs (Chrzanowska-Wodnicka and Burridge, 1996), whereas RhoA inactivation by p190RhoGAP promotes cell spreading and migration (Arthur and Burridge, 2001). Consistent with the notion that elevated Rho is responsible for the defects in FA dynamics and cell spreading seen in our *Fak*-null keratinocytes, these defects could be largely suppressed by inhibitors of ROCK or myosin II. MLCK inhibition also had an effect, suggesting that multiple pathways are involved in regulating FA-mediated tension.

In fibroblasts, MLCK can be inactivated by PAK (Sanders et al., 1999), and a constitutively active form of PAK causes dissolution of stress fibers and FA reorganization (Manser et al., 1997). Our finding that endogenous phosphorylated (active) PAK is diminished at FAs in *Fak*-null keratinocytes extends these earlier inverse connections between activated PAK and MLCK-mediated tension. Moreover, when considered with the knowledge that PKL, β PIX, and PAK form a complex that binds to PXN at FAs (Frost et al., 1998; Manser et al., 1998; Turner et al., 1999; Zhao et al., 2000; West et al., 2001; Webb et al., 2004; Nayal et al., 2006), our data provide compelling evidence

that inactivation of the PXN-PAK-MLCK pathway in the absence of FAK activity might lead to increased tension and larger, less dynamic FAs.

Our findings point to a function for FAK in localizing PKL-PIX-PAK to FAs to ease MLCK activity. How FAK regulates PKL-PIX-PAK localization remains unclear, but we do see a reduction in PKL at *Fak*-null FAs, which could account for the markedly reduced PAK activity at these sites. It was recently shown that PKL can be cooperatively phosphorylated on multiple tyrosine residues by FAK and Src to promote PKL localization to FAs (Brown et al., 2005). Overall, these data support a model whereby FAK promotes the recruitment and activation of PAK at FAs to suppress MLCK activity. This adds an additional way in which activation of FAK tips the balance in favor of the unphosphorylated (inactive) form of MLC to reduce tensile stress fibers associated with FA dynamics (Fig. S5 B).

FAK, FA dynamics, directed cell migration, and cellular context

The migratory behavior of cells is complex and can be altered by a variety of parameters. Providing a structural link between the matrix and the cytoskeleton are integrins and their associated scaffolding and signaling molecules. This machinery couples matrix stiffness to cellular tension and is a crucial determinant of cell motility (Gupton and Waterman-Storer, 2006). Our studies provide functional evidence to reinforce the notion that FAK is an essential component of FA distribution and dynamics

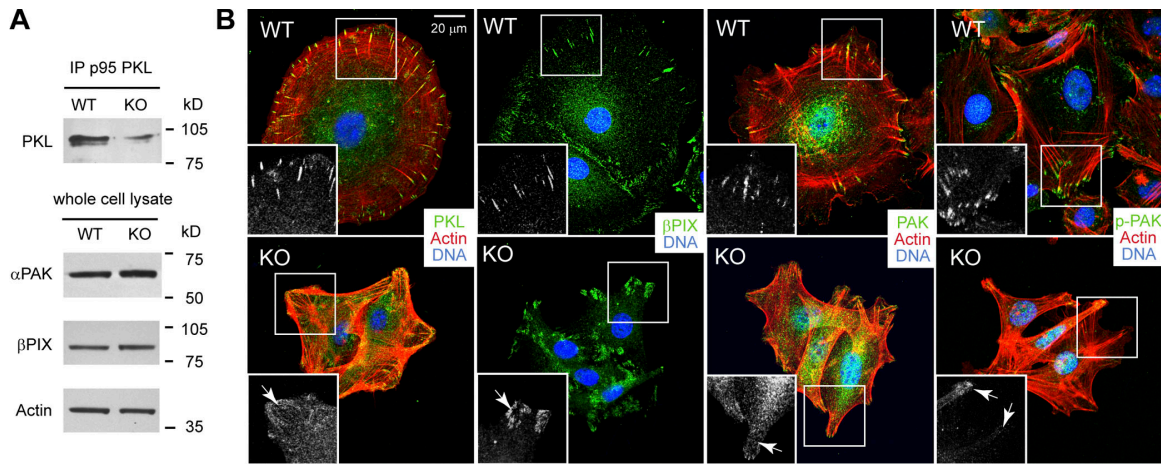


Figure 10. **In the absence of FAK, PKL and PAK activity are diminished at FAs.** (A) Immunoblot analyses reveal reduced levels of PKL without major differences in levels of PAK or PAK-interacting guanine nucleotide exchange factor (β PIX; actin is control). (B) Immunofluorescence microscopy shows that PKL, β PIX, PAK, and phosphorylated (active) PAK (p-PAK) localize at FAs in WT MKs, whereas *Fak* KO FAs still contain β PIX but show severely reduced staining for PKL, PAK, and p-PAK. Phalloidin (red) marks F-actin, and DAPI (blue) marks chromatin.

within cells. In the absence of FAK, the small central FAs diminished dramatically in number and were replaced by large peripheral focal contacts. Kinetic studies on FA assembly and disassembly indicate that FAK's major requirement resides in promoting FA disassembly, although moderate alterations in assembly rates were observed (this study; Webb et al., 2004).

The defects in directed migration of cells exiting from *Fak*-null skin explants were striking and graphically revealed the physiological consequences to tension-induced perturbations in actin organization. The reduced FA dynamics also appeared to contribute, as robust FAs were misoriented in FAK-deficient explants. The pronounced targeting of microtubules to these FAs is consistent with prior studies showing that microtubules grow along actin stress fibers (Kodama et al., 2003; Rodriguez et al., 2003). This finding suggests that despite their robust appearance, these FAs are still able to undergo the microtubule-mediated turnover first described by Small et al. (2002) (for review see Kaverina et al., 2002). Future studies will be necessary to explore these connections in depth.

The grossly perturbed epidermal migration that we observed is consistent with both the abnormalities seen in hair follicle morphogenesis and the resistance of *Fak*-null skin to tumorigenesis and metastasis (McLean et al., 2004; Essayem et al., 2006). Although postnatal ablation of FAK in the skin epithelium resulted in no significant wound healing defects (McLean et al., 2004; Essayem et al., 2006; unpublished data), delays in epidermal wound closure were noted in β 1-null skin (Grose et al., 2002). We surmise that our enhanced ability to detect and monitor migration differences in skin explants arises from an increase in keratinocyte mobilization in vitro, where growth conditions are optimal and hemidesmosomal adhesion to ECM is reduced (Fuchs and Raghavan, 2002).

It is also noteworthy that FAK's specific functions may vary both with changes in microenvironment and inherent differences in cell types. The importance of these contexts is underscored by *Fak*-null-mediated basement membrane

assembly defects, which were observed in cerebellum (Beggs et al., 2003) but not in embryonic fibroblasts (Ilic et al., 1995) or skin epidermis (this study). Furthermore, although both *Fak*-null primary keratinocytes and immortalized *Fak* embryonic fibroblasts exhibit elaborate arrays of stress fibers and FAs that impair migration, FAK-deficient HeLa cells display elevated Rac rather than Rho activity and show enhanced rather than impaired migration (Ilic et al., 1995; Webb et al., 2004; Yano et al., 2004; Braren et al., 2006). In contrast, *Fak*-null endothelial cells spread poorly and display aberrant lamellipodial extensions and altered actin cytoskeleton, and yet surprisingly, they exhibit no obvious perturbations in polarized migration during vascularigenesis in tissue explants (Braren et al., 2006). Finally, *Fak* mutant fruit flies, which do not express a *Pyk2*-like gene, are surprisingly viable and fertile and show no defects in either integrin function or cell migration (Grabbe et al., 2004).

Summary

In closing, our analysis of FA dynamics in primary keratinocytes lacking FAK function has provided new insights and strengthened prior notions as to how FAK activity converges on the constellation of pathways that regulate cytoskeletal dynamics and balance FA assembly and disassembly in cells. Our findings are particularly interesting in the context of recent in vivo studies, which showed that oncogenic transformation is severely reduced in skin with reduced or abrogated FAK function (McLean et al., 2001, 2004). In this regard, FA signaling has recently been implicated in oncogenic transformation and activated FAK is a well-established marker for both transformation and metastasis. The identification of FAK-mediated alterations in several specific FA-associated proteins, cytoskeletal changes, and FA dynamics now illuminates several potential molecular pathways by which FA signaling might result in oncogenic transformation. These new findings provide fertile ground for future investigations in this arena.

Materials and methods

Mice and tissue culture

FAK floxed mice [Beggs et al., 2003], *K14-Cre* mice [Vasioukhin et al., 1999], and *K14-GFPactin* mice [Vaezi et al., 2002] have been described. Homozygous *FAK floxed*; *K14-Cre* and *FAK floxed*; and *K14-cre*, *K14-GFPactin* animals were generated by mating, and their genotypes were determined by PCR. Primary mouse keratinocytes (MKs) were isolated from the epidermis of newborn mice using trypsin, after prior separation of the epidermis from the dermis by a 2-h dispase treatment. MKs were plated on either mitomycin C-treated 3T3 fibroblast feeder cells or onto different ECM components. Cells were cultured in E-media supplemented with 15% serum and a final concentration of 0.05 mM Ca²⁺ [Rheinwald and Green, 1977].

Cell adhesion assays were performed as described previously [Raghavan et al., 2003]. Wells were coated using 10 µg/ml FN, 10 µg/ml laminin-1, 10 µg/ml collagen-4, and poly-L-lysine. Cell spreading assays were performed by plating MKs at low density on FN-coated coverslips. Cells were fixed 2, 12, 24, or 36 h after plating and stained with TRITC-phalloidin and DAPI. Suppression of tension signaling during spreading was analyzed by plating MKs at low density on FN-coated coverslips for 12 h in E-media containing 0.05 mM Ca²⁺. After 12 h, the medium was exchanged for medium containing 5 µM ML7 (BIOMOL Research Laboratories, Inc.) or 5 µM Y27632 (Calbiochem) and incubated for an additional 12 or 24 h before fixation. For ectopic expression and rescue experiments, MKs were transfected with RFPzyxin (M. Beckerle, University of Utah, Salt Lake City, UT), pEGFP-PXN (E. Marcantonio, Columbia University Medical Center, New York, NY), and pBABE-FAK (Y. Pylayeva and F. Giancotti, Memorial Sloan-Kettering Cancer Center, New York, NY) using Fugene6 (Roche Applied Science).

FRAP and FA assembly/disassembly measurements

Kinetics of FA assembly and disassembly were performed as previously described [Webb et al., 2004]. MKs were plated on FN-coated dishes (MatTek) in media containing 0.05 mM Ca²⁺ and transfected with GFP-PXN. Time series were acquired on a spinning-disc confocal microscope equipped with a 100× α -plane fluor (1.45 oil) lens and an EM charge-coupled device camera (Hamamatsu). The rate constants for FA assembly and disassembly were obtained by calculating the slope of relative fluorescence intensity increases or decreases of individual FAs on a semilogarithmic scale against time.

For FRAP experiments, MKs were plated on FN-coated 3.5-cm dishes in media containing 0.05 mM Ca²⁺ and transfected with GFP-PXN. FRAP experiments were performed on a microscope (DeltaVision; Stress Photonics) equipped with a 60× Plan APO N (1.42 oil) objective. The refractive index of the oil was 1.514 [Applied Precision]. Five pre-bleach events were acquired followed by a 1-s bleach event. Fluorescence recovery was recorded for 120 s after photobleaching (71 frames), and data from these photokinetic experiments were analyzed using DeltaVision software.

Quantification of FA size, relative staining intensity, and distance from the cell periphery

MKs were fixed and stained with mouse anti-VIN and FITC anti-mouse antibodies to label FAs, TRITC-phalloidin to determine the cell boundaries, and DAPI. Pictures were acquired on a confocal microscope (510 META; Carl Zeiss MicroImaging, Inc.) at 63× C-Apochromat (1.2 W Korr) objective on a 12-bit scale. FA characteristics were quantified using MetaMorph 7 (Universal Imaging Corp.). An integrated morphometric analysis was performed on thresholded images to select classified objects of a size range of $0.1 \leq N \leq 1E08$ as FAs based on the anti-VIN staining.

The distance between all FAs and the cell periphery was determined by selecting the cell boundaries based on the rhodamine-phalloidin staining for individual cells, conversion to a binary image, and inversion of the binary image. Subsequently, an euclidean distance map was generated from the inverted image. The euclidean distance map displays the closest distance of any point within the object (foreground) and the area surrounding the object (background) as an intensity value. Regions demarcating individual FAs of the given cell were transferred on the euclidean distance map where the minimum intensity of each individual FA corresponds to its closest distance to the cell edge.

Migration assays

Explant outgrowth migration assays were performed as described previously [Raghavan et al., 2003] with minor modifications. In brief, explants

were cut using a 3-mm dermal biopsy punch (Miltex), placed on FN-coated 35-mm, glass-bottomed plates (MatTek), and submerged in E-media containing 0.6 mM Ca²⁺. For video microscopy, explant cultures were incubated with E-media containing 0.6 mM Ca²⁺ and 50 mM Hepes buffer, pH 7.

Transwell migration assays were performed on 24-well plates. The underside of each well was coated with 10 µg/ml FN and placed atop fibroblast-conditioned E-media containing 0.05 mM Ca²⁺. Primary MKs were freshly isolated, and a total of 50,000 cells/well were plated in 100 µl E-medium containing 0.05 mM Ca²⁺. 12 h later, cells were washed off the top membrane and fixed on the bottom membrane. Cells were stained using hematoxylin and eosin and counted under the microscope.

Immunofluorescence and immunoprecipitations

Tissues or cells were subjected to immunofluorescence microscopy and analyzed using a LSM 510 confocal microscope or a spinning-disc confocal microscope (PerkinElmer). mAbs used were as follows: rat anti- β 1 (1:100; Chemicon), CD29 (9EG7; BD Biosciences), α 2 (1:50; BD Biosciences), α 6 (1:50; BD Biosciences), α v β 6 (1:100; Chemicon), β 4 (1:50; BD Biosciences), β -tubulin (1:200; Sigma-Aldrich), mouse anti-VIN (Sigma-Aldrich), FAK (Upstate Biotechnology), PXN (Upstate Biotechnology), ILK (Upstate Biotechnology), Src (Upstate Biotechnology), PKL (BD Bioscience), MLC (Sigma-Aldrich), phosphotyrosine (4G10; Upstate Biotechnology), E-cadherin (Developmental Studies Hybridoma Bank), Erk1/2 (Sigma-Aldrich), and actin (Sigma-Aldrich). Rabbit polyclonal antibodies used were as follows: laminin 5 (1:200; a gift from R. Burgeson, Massachusetts General Hospital and Harvard Medical School, Charleston, MA), AKT (Cell Signaling), phospho-AKT (Cell Signaling), pY418-Src (Biosource International), β PIX (Chemicon), pS19-MLC (Cell Signaling), PAK (N-20; Santa Cruz Biotechnology, Inc.), phospho-PAK1 (Ser199/204)/PAK2 (Ser192/197) (Cell Signaling), pY397-FAK (Biosource International), PYK2 (BD Bioscience), pY402-PYK2 (Abcam), p42/44 (Cell Signaling), MYPT1 (Upstate Biotechnology), phospho-MYPT1 (Upstate Biotechnology), and p190RhoGAP (Sigma-Aldrich). Primary antibodies were used at 1:100 unless specified otherwise. Fluorescent-conjugated secondary antibodies rhodamine RedX (Jackson ImmunoResearch Laboratories) and Alexa Fluor (Invitrogen) were used at 1:500. Additional reagents used were TRITC/FITC phalloidin (1:1,000; Sigma-Aldrich), DAPI (1:5,000; Sigma-Aldrich), and pEGFP-tubulin (CLONTECH Laboratories, Inc.).

For immunoprecipitations, cells were lysed in NP-40 buffer (50 mM Tris, pH 7.5, 150 mM NaCl, 2 mM EDTA, 1% NP-40, 0.5% sodium deoxycholate, protease inhibitor cocktail, 2 mM PMSF, 25 mM NaF, and 1 mM sodium orthovanadate). Protein concentration was determined using the protein assay (Bio-Rad Laboratories, Inc.). Immunoprecipitations were performed from cell lysates containing 1 mg of total protein. Cell lysates were precleared for 1 h using protein G-Sepharose beads before incubation with primary antibodies. Primary antibodies were used at a concentration of 2–4 µg/ml Ig according to manufacturers' recommendations and incubated for 4 h at 4°C. Protein complexes were collected by incubation with protein G-Sepharose, washed five times with NP-40 wash buffer (50 mM Tris, pH 7.5, 150 mM NaCl, 2 mM EDTA, 0.1% NP-40, 0.05% sodium deoxycholate, protease inhibitor cocktail, 2 mM PMSF, 25 mM NaF, and 1 mM sodium orthovanadate), and resuspended in 3× SDS sample buffer.

Immunoblots

Proteins were separated by electrophoresis on 6–10% PAGE gels or 4–12% gradient gels (Invitrogen), transferred to nitrocellulose membrane, and subjected to immunoblotting. Membranes were blocked for 30 min with 5% nonfat milk in PBS containing 0.1% Tween 20, except for phosphoantibodies and MLC, where membranes were blocked for 30 min with 3% BSA in PBS containing 0.1% Tween 20. Primary antibodies were generally used at a concentration of 1:1,000, and HRP-coupled secondary antibodies were used at 1:3,000. Immunoblots were developed using standard ECL (GE Healthcare) or Super Signal West Pico substrate (Pierce Chemical Co.).

FACS analyses

Freshly isolated primary MKs were washed twice with PBS blocking solution containing 2% FCS at 4°C. Cells were resuspended and incubated in primary antibody (1:50) in blocking solution for 30 min at 4°C, washed three times with blocking solution, and incubated with PE-conjugated secondary antibodies (1:100) for 30 min at 4°C. Cells were washed three times in blocking solution and resuspended in blocking solution containing propidium iodide. FACS analyses were performed on a FACScan (Becton

Dickinson). BrdU incorporation was quantified by FACS using a FITC BrdU FACS Flow kit (BD Biosciences) following the manufacturer's instructions.

EM

Tissues were fixed for >1 h in 2% glutaraldehyde, 4% formaldehyde, and 2 mM CaCl₂ in 0.05 M sodium cacodylate buffer and then processed for Epon embedding. Samples were visualized with a transmission electron microscope (Tecnai 12-G2; FEI). For hemidesmosome quantitation, EM images were taken with a digital camera (model XR60; Advanced Microscopy Techniques Corp.) at a magnification of 49,000 \times . A total of 150 images were randomly taken at sites of the dermal-epidermal boundary for each experimental model. Total continuous membrane length and individual hemidesmosomes' lengths along the plasma membrane were measured using ImageJ (NIH).

Statistical analysis

Statistical analysis was performed using OriginLab 7.5 software. Box-and-whisker blots are used to describe the entire population without assumptions on the statistical distribution. A *t* test was used to assess the statistical significance of differences between two experimental conditions, and analysis of variance in combination with a Tukey post hoc test was used to compare multiple experimental conditions.

Online supplemental material

Fig. S1 describes defects in hair follicle morphogenesis in mice conditionally mutant for FAK in the skin epithelium. Fig. S2 is a schematic representation of a box-and-whisker diagram. Fig. S3 shows the convergence of stress fibers and microtubules at FAs. Fig. S4 illustrates the distribution, relative VIN staining intensity, and size of FAs after treatment with small molecule inhibitors of tension-signaling components. Fig. S5 summarizes the presented data in a schematic model. Videos 1 and 2 are time-lapse videos illustrating the dynamics of FAs (RFPzyxin) and the actin cytoskeleton (GFPactin) in WT and KO keratinocytes. Video 3 is a time-lapse video of GFPactin in keratinocytes migrating out of WT and KO epidermal explants. Video 4 is a time-lapse video of GFPTubulin. Video 5 is a time-lapse video of EB1-GFP in WT and KO keratinocytes. Online supplemental material is available at <http://www.jcb.org/cgi/content/full/jcb.200608010/DC1>.

We thank Eva Gonzalez, Terry Lechler, Agnes Kobiela, Danelle Devenport, and Scott Williams for discussions and critical reading of the manuscript; M. Beckerle, R. Burgeson, E.E. Marcantonio, Yuliya Pylayeva, Filippo Giancotti, and Y. Mimori-Kiyosue for reagents; and Alison North and Mathieu Marchand from the Rockefeller Bioimaging Facility and Penny Tavormina (Molecular Devices) for helpful suggestions on quantitative image acquisition and analysis.

This work was supported by a grant from the National Institutes of Health (R01-AR27883). M. Schober is the recipient of a postdoctoral fellowship from the Jane Coffin Childs Memorial Fund for Medical Research. E. Fuchs is an investigator of the Howard Hughes Medical Institute.

Submitted: 2 August 2006

Accepted: 25 January 2007

References

Arthur, W.T., and K. Burridge. 2001. RhoA inactivation by p190RhoGAP regulates cell spreading and migration by promoting membrane protrusion and polarity. *Mol. Biol. Cell.* 12:2711–2720.

Arthur, W.T., L.A. Petch, and K. Burridge. 2000. Integrin engagement suppresses RhoA activity via a c-Src-dependent mechanism. *Curr. Biol.* 10:719–722.

Astier, A., H. Avraham, S.N. Manie, J. Groopman, T. Canty, S. Avraham, and A.S. Freedman. 1997. The related adhesion focal tyrosine kinase is tyrosine-phosphorylated after beta1-integrin stimulation in B cells and binds to p130cas. *J. Biol. Chem.* 272:228–232.

Avizienyte, E., A.W. Wyke, R.J. Jones, G.W. McLean, M.A. Westhoff, V.G. Brunton, and M.C. Frame. 2002. Src-induced de-regulation of E-cadherin in colon cancer cells requires integrin signalling. *Nat. Cell Biol.* 4:632–638.

Beggs, H.E., D. Schahin-Reed, K. Zang, S. Goebels, K.A. Nave, J. Gorski, K.R. Jones, D. Sretavan, and L.F. Reichardt. 2003. FAK deficiency in cells contributing to the basal lamina results in cortical abnormalities resembling congenital muscular dystrophies. *Neuron.* 40:501–514.

Bershadsky, A., A. Chausovsky, E. Becker, A. Lyubimova, and B. Geiger. 1996. Involvement of microtubules in the control of adhesion-dependent signal transduction. *Curr. Biol.* 6:1279–1289.

Bhatt, A., I. Kaverina, C. Otey, and A. Huttenlocher. 2002. Regulation of focal complex composition and disassembly by the calcium-dependent protease calpain. *J. Cell Sci.* 115:3415–3425.

Billuart, P., C.G. Winter, A. Maresh, X. Zhao, and L. Luo. 2001. Regulating axon branch stability: the role of p190 RhoGAP in repressing a retraction signaling pathway. *Cell.* 107:195–207.

Brakebusch, C., R. Grose, F. Quondamatteo, A. Ramirez, J.L. Jorcano, A. Pirro, M. Svensson, R. Herken, T. Sasaki, R. Timpl, et al. 2000. Skin and hair follicle integrity is crucially dependent on beta 1 integrin expression on keratinocytes. *EMBO J.* 19:3990–4003.

Braren, R., H. Hu, Y.H. Kim, H.E. Beggs, L.F. Reichardt, and R. Wang. 2006. Endothelial FAK is essential for vascular network stability, cell survival, and lamellipodial formation. *J. Cell Biol.* 172:151–162.

Brouns, M.R., S.F. Matheson, and J. Settleman. 2001. p190 RhoGAP is the principal Src substrate in brain and regulates axon outgrowth, guidance and fasciculation. *Nat. Cell Biol.* 3:361–367.

Brown, M.C., L.A. Cary, J.S. Jamieson, J.A. Cooper, and C.E. Turner. 2005. Src and FAK kinases cooperate to phosphorylate paxillin kinase linker, stimulate its focal adhesion localization, and regulate cell spreading and protrusiveness. *Mol. Biol. Cell.* 16:4316–4328.

Chen, L.M., D. Bailey, and C. Fernandez-Valle. 2000. Association of beta 1 integrin with focal adhesion kinase and paxillin in differentiating Schwann cells. *J. Neurosci.* 20:3776–3784.

Chrzanoska-Wodnicka, M., and K. Burridge. 1996. Rho-stimulated contractility drives the formation of stress fibers and focal adhesions. *J. Cell Biol.* 133:1403–1415.

DiPersio, C.M., K.M. Hodivala-Dilke, R. Jaenisch, J.A. Kreidberg, and R.O. Hynes. 1997. α 3 β 1 integrin is required for normal development of the epidermal basement membrane. *J. Cell Biol.* 137:729–742.

Dowling, J., Q.C. Yu, and E. Fuchs. 1996. β 4 integrin is required for hemidesmosome formation, cell adhesion and cell survival. *J. Cell Biol.* 134:559–572.

Dumenil, G., P. Sansonetti, and G. Tran Van Nhieu. 2000. Src tyrosine kinase activity down-regulates Rho-dependent responses during Shigella entry into epithelial cells and stress fibre formation. *J. Cell Sci.* 113:71–80.

Essayem, S., B. Kovacic-Milivojevic, C. Baumbusch, S. McDonagh, G. Dolganov, K. Howerton, N. Larocque, T. Mauro, A. Ramirez, D.M. Ramos, et al. 2006. Hair cycle and wound healing in mice with a keratinocyte-restricted deletion of FAK. *Oncogene.* 25:1081–1089.

Etienne-Manneville, S., and A. Hall. 2002. Rho GTPases in cell biology. *Nature.* 420:629–635.

Ezratty, E.J., M.A. Partridge, and G.G. Gundersen. 2005. Microtubule-induced focal adhesion disassembly is mediated by dynamin and focal adhesion kinase. *Nat. Cell Biol.* 7:581–590.

Fincham, V.J., A. Chudleigh, and M.C. Frame. 1999. Regulation of p190 RhoGAP by v-Src is linked to cytoskeletal disruption during transformation. *J. Cell Sci.* 112:947–956.

Frost, J.A., A. Khokhlatchev, S. Stippes, M.A. White, and M.H. Cobb. 1998. Differential effects of PAK1-activating mutations reveal activity-dependent and -independent effects on cytoskeletal regulation. *J. Biol. Chem.* 273:28191–28198.

Fuchs, E., and S. Raghavan. 2002. Getting under the skin of epidermal morphogenesis. *Nat. Rev. Genet.* 3:199–209.

Fuchs, E., J. Dowling, J. Segre, S.H. Lo, and Q.C. Yu. 1997. Integrators of epidermal growth and differentiation: distinct functions for beta 1 and beta 4 integrins. *Curr. Opin. Genet. Dev.* 7:672–682.

Georges-Labouesse, E., N. Messaddeq, G. Yehia, L. Cadalbert, A. Dierich, and M. Le Meur. 1996. Absence of integrin alpha 6 leads to epidermolysis bullosa and neonatal death in mice. *Nat. Genet.* 13:370–373.

Giancotti, F.G., and G. Tarone. 2003. Positional control of cell fate through joint integrin/receptor protein kinase signaling. *Annu. Rev. Cell Dev. Biol.* 19:173–206.

Gismondi, A., L. Bisogno, F. Mainiero, G. Palmieri, M. Piccoli, L. Frati, and A. Santoni. 1997. Proline-rich tyrosine kinase-2 activation by beta 1 integrin fibronectin receptor cross-linking and association with paxillin in human natural killer cells. *J. Immunol.* 159:4729–4736.

Grabbe, C., C.G. Zervas, T. Hunter, N.H. Brown, and R.H. Palmer. 2004. Focal adhesion kinase is not required for integrin function or viability in *Drosophila*. *Development.* 131:5795–5805.

Grose, R., C. Hutter, W. Bloch, I. Thorey, F.M. Watt, R. Fassler, C. Brakebusch, and S. Werner. 2002. A crucial role of beta 1 integrins for keratinocyte migration in vitro and during cutaneous wound repair. *Development.* 129:2303–2315.

Gupton, S.L., and C.M. Waterman-Storer. 2006. Spatiotemporal feedback between actomyosin and focal-adhesion systems optimizes rapid cell migration. *Cell.* 125:1361–1374.

- Hannigan, G.E., C. Leung-Hagesteijn, L. Fitz-Gibbon, M.G. Copolino, G. Radeva, J. Filmus, J.C. Bell, and S. Dedhar. 1996. Regulation of cell adhesion and anchorage-dependent growth by a new beta 1-integrin-linked protein kinase. *Nature*. 379:91–96.
- Hannigan, G., A.A. Troussard, and S. Dedhar. 2005. Integrin-linked kinase: a cancer therapeutic target unique among its ILK. *Nat. Rev. Cancer*. 5:51–63.
- Holinstat, M., N. Knezevic, M. Broman, A.M. Samarel, A.B. Malik, and D. Mehta. 2006. Suppression of RhoA activity by focal adhesion kinase-induced activation of p190RhoGAP: role in regulation of endothelial permeability. *J. Biol. Chem.* 281:2296–2305.
- Hsia, D.A., S.K. Mitra, C.R. Hauck, D.N. Streblow, J.A. Nelson, D. Ilic, S. Huang, E. Li, G.R. Nemerow, J. Leng, et al. 2003. Differential regulation of cell motility and invasion by FAK. *J. Cell Biol.* 160:753–767.
- Hynes, R.O. 2002. Integrins: bidirectional, allosteric signaling machines. *Cell*. 110:673–687.
- Ilic, D., Y. Furuta, S. Kanazawa, N. Takeda, K. Sobue, N. Nakatsuji, S. Nomura, J. Fujimoto, M. Okada, and T. Yamamoto. 1995. Reduced cell motility and enhanced focal adhesion contact formation in cells from FAK-deficient mice. *Nature*. 377:539–544.
- Janes, S.M., and F.M. Watt. 2006. New roles for integrins in squamous-cell carcinoma. *Nat. Rev. Cancer*. 6:175–183.
- Kaverina, I., K. Rottner, and J.V. Small. 1998. Targeting, capture, and stabilization of microtubules at early focal adhesions. *J. Cell Biol.* 142:181–190.
- Kaverina, I., O. Krylyshkina, and J.V. Small. 1999. Microtubule targeting of substrate contacts promotes their relaxation and dissociation. *J. Cell Biol.* 146:1033–1044.
- Kaverina, I., O. Krylyshkina, and J.V. Small. 2002. Regulation of substrate adhesion dynamics during cell motility. *Int. J. Biochem. Cell Biol.* 34:746–761.
- Kodama, A., I. Karakesisoglou, E. Wong, A. Vaezi, and E. Fuchs. 2003. ACF7: an essential integrator of microtubule dynamics. *Cell*. 115:343–354.
- Legate, K.R., E. Montanez, O. Kudlacek, and R. Fassler. 2006. ILK, PINCH and parvin: the tIPP of integrin signalling. *Nat. Rev. Mol. Cell Biol.* 7:20–31.
- Manser, E., H.Y. Huang, T.H. Loo, X.Q. Chen, J.M. Dong, T. Leung, and L. Lim. 1997. Expression of constitutively active alpha-PAK reveals effects of the kinase on actin and focal complexes. *Mol. Cell Biol.* 17:1129–1143.
- Manser, E., T.H. Loo, C.G. Koh, Z.S. Zhao, X.Q. Chen, L. Tan, I. Tan, T. Leung, and L. Lim. 1998. PAK kinases are directly coupled to the PIX family of nucleotide exchange factors. *Mol. Cell*. 1:183–192.
- Matsumura, F. 2005. Regulation of myosin II during cytokinesis in higher eukaryotes. *Trends Cell Biol.* 15:371–377.
- McLean, G.W., K. Brown, M.I. Arbuckle, A.W. Wyke, T. Pikkarainen, E. Ruoslahti, and M.C. Frame. 2001. Decreased focal adhesion kinase suppresses papilloma formation during experimental mouse skin carcinogenesis. *Cancer Res.* 61:8385–8389.
- McLean, G.W., N.H. Komiyama, B. Serrels, H. Asano, L. Reynolds, F. Conti, K. Hodivala-Dilke, D. Metzger, P. Chambon, S.G. Grant, and M.C. Frame. 2004. Specific deletion of focal adhesion kinase suppresses tumor formation and blocks malignant progression. *Genes Dev.* 18:2998–3003.
- McLean, G.W., N.O. Carragher, E. Avizienyte, J. Evans, V.G. Brunton, and M.C. Frame. 2005. The role of focal-adhesion kinase in cancer—a new therapeutic opportunity. *Nat. Rev. Cancer*. 5:505–515.
- Miranti, C.K., and J.S. Brugge. 2002. Sensing the environment: a historical perspective on integrin signal transduction. *Nat. Cell Biol.* 4:E83–E90.
- Nayal, A., D.J. Webb, C.M. Brown, E.M. Schaefer, M. Vicente-Manzanares, and A.R. Horwitz. 2006. Paxillin phosphorylation at Ser273 localizes a GIT1-PIX-PAK complex and regulates adhesion and protrusion dynamics. *J. Cell Biol.* 173:587–589.
- Owens, D.M., S. Broad, X. Yan, S.A. Benitah, and F.M. Watt. 2005. Suprabasal alpha 5 beta1 integrin expression stimulates formation of epidermal squamous cell carcinomas without disrupting TGFbeta signaling or inducing spindle cell tumors. *Mol. Carcinog.* 44:60–66.
- Raghavan, S., C. Bauer, G. Mundscha, Q. Li, and E. Fuchs. 2000. Conditional ablation of beta1 integrin in skin: severe defects in epidermal proliferation, basement membrane formation, and hair follicle invagination. *J. Cell Biol.* 150:1149–1160.
- Raghavan, S., A. Vaezi, and E. Fuchs. 2003. A role for alphabeta1 integrins in focal adhesion function and polarized cytoskeletal dynamics. *Dev. Cell*. 5:415–427.
- Ren, X.D., W.B. Kiesses, D.J. Sieg, C.A. Otey, D.D. Schlaepfer, and M.A. Schwartz. 2000. Focal adhesion kinase suppresses Rho activity to promote focal adhesion turnover. *J. Cell Sci.* 113:3673–3678.
- Rheinwald, J.G., and H. Green. 1977. Epidermal growth factor and the multiplication of cultured human epidermal keratinocytes. *Nature*. 265:421–424.
- Rodriguez, O.C., A.W. Schaefer, C.A. Mandato, P. Forscher, W.M. Bement, and C.M. Waterman-Storer. 2003. Conserved microtubule-actin interactions in cell movement and morphogenesis. *Nat. Cell Biol.* 5:599–609.
- Sanders, L.C., F. Matsumura, G.M. Bokoch, and P. de Lanerolle. 1999. Inhibition of myosin light chain kinase by p21-activated kinase. *Science*. 283:2083–2085.
- Schaller, M.D., J.D. Hildebrand, J.D. Shannon, J.W. Fox, R.R. Vines, and J.T. Parsons. 1994. Autophosphorylation of the focal adhesion kinase, pp125FAK, directs SH2-dependent binding of pp60src. *Mol. Cell Biol.* 14:1680–1688.
- Schaller, M.D., C.A. Otey, J.D. Hildebrand, and J.T. Parsons. 1995. Focal adhesion kinase and paxillin bind to peptides mimicking beta integrin cytoplasmic domains. *J. Cell Biol.* 130:1181–1187.
- Schwartz, M.A., and M.H. Ginsberg. 2002. Networks and crosstalk: integrin signalling spreads. *Nat. Cell Biol.* 4:E65–E68.
- Shen, T.L., A.Y. Park, A. Alcaraz, X. Peng, I. Jang, P. Koni, R.A. Flavell, H. Gu, and J.L. Guan. 2005. Conditional knockout of focal adhesion kinase in endothelial cells reveals its role in angiogenesis and vascular development in late embryogenesis. *J. Cell Biol.* 169:941–952.
- Small, J.V., B. Geiger, I. Kaverina, and A. Bershadsky. 2002. How do microtubules guide migrating cells? *Nat. Rev. Mol. Cell Biol.* 3:957–964.
- Tilghman, R.W., J.K. Slack-Davis, N. Sergina, K.H. Martin, M. Iwanicki, E.D. Hershey, H.E. Beggs, L.F. Reichardt, and J.T. Parsons. 2005. Focal adhesion kinase is required for the spatial organization of the leading edge in migrating cells. *J. Cell Sci.* 118:2613–2623.
- Tukey, J.W. 1977. *Exploratory Data Analysis*. Addison-Wesley, Reading, MA. 688 pp.
- Turner, C.E., M.C. Brown, J.A. Perrotta, M.C. Riedy, S.N. Nikolopoulos, A.R. McDonald, S. Bagrodia, S. Thomas, and P.S. Leventhal. 1999. Paxillin LD4 motif binds PAK and PIX through a novel 95-kD ankyrin repeat, ARF-GAP protein: a role in cytoskeletal remodeling. *J. Cell Biol.* 145:851–863.
- Vaezi, A., C. Bauer, V. Vasioukhin, and E. Fuchs. 2002. Actin cable dynamics and Rho/Rock orchestrate a polarized cytoskeletal architecture in the early steps of assembling a stratified epithelium. *Dev. Cell*. 3:367–381.
- van der Neut, R., P. Krimpenfort, J. Calafat, C.M. Niessen, and A. Sonnenberg. 1996. Epithelial detachment due to absence of hemidesmosomes in integrin beta 4 null mice. *Nat. Genet.* 13:366–369.
- Vasioukhin, V., L. Degenstein, B. Wise, and E. Fuchs. 1999. The magical touch: genome targeting in epidermal stem cells induced by tamoxifen application to mouse skin. *Proc. Natl. Acad. Sci. USA*. 96:8551–8556.
- Watt, F.M. 2002. Role of integrins in regulating epidermal adhesion, growth and differentiation. *EMBO J.* 21:3919–3926.
- Webb, D.J., K. Donais, L.A. Whitmore, S.M. Thomas, C.E. Turner, J.T. Parsons, and A.F. Horwitz. 2004. FAK-Src signalling through paxillin, ERK and MLCK regulates adhesion disassembly. *Nat. Cell Biol.* 6:154–161.
- West, K.A., H. Zhang, M.C. Brown, S.N. Nikolopoulos, M.C. Riedy, A.F. Horwitz, and C.E. Turner. 2001. The LD4 motif of paxillin regulates cell spreading and motility through an interaction with paxillin kinase linker (PKL). *J. Cell Biol.* 154:161–176.
- Wilhelmsen, K., S.H. Litjens, and A. Sonnenberg. 2006. Multiple functions of the integrin alpha6beta4 in epidermal homeostasis and tumorigenesis. *Mol. Cell Biol.* 26:2877–2886.
- Wu, X., B. Gan, Y. Yoo, and J.L. Guan. 2005. FAK-mediated src phosphorylation of endophilin A2 inhibits endocytosis of MT1-MMP and promotes ECM degradation. *Dev. Cell*. 9:185–196.
- Yano, H., Y. Mazaki, K. Kurokawa, S.K. Hanks, M. Matsuda, and H. Sabe. 2004. Roles played by a subset of integrin signaling molecules in cadherin-based cell–cell adhesion. *J. Cell Biol.* 166:283–295.
- Zhao, Z.S., E. Manser, T.H. Loo, and L. Lim. 2000. Coupling of PAK-interacting exchange factor PIX to GIT1 promotes focal complex disassembly. *Mol. Cell Biol.* 20:6354–6363.